



**NIST Technical Note
NIST TN 2245**

Measuring Water Flow Rate for a Fire Hose Using a Wireless Sensor Network for Smart Fire Fighting

An Update Using Various Hose Conditions

Christopher U. Brown
Gregory W. Vogl
Wai Cheong Tam

This publication is available free of charge from:
<https://doi.org/10.6028/NIST.TN.2245>

**NIST Technical Note
NIST TN 2245**

Measuring Water Flow Rate for a Fire Hose Using a Wireless Sensor Network for Smart Fire Fighting

An Update Using Various Hose Conditions

Christopher U. Brown
Wai Cheong Tam
*Fire Research Division
Engineering Laboratory*

Gregory W. Vogl
*Intelligent Systems Division
Engineering Laboratory*

This publication is available free of charge from:
<https://doi.org/10.6028/NIST.TN.2245>

January 2023



U.S. Department of Commerce
Gina M. Raimondo, Secretary

National Institute of Standards and Technology
Laurie E. Locascio, NIST Director and Under Secretary of Commerce for Standards and Technology

NIST TN 2245
January 2023

Certain commercial entities, equipment, or materials may be identified in this document in order to describe an experimental procedure or concept adequately. Such identification is not intended to imply recommendation or endorsement by the National Institute of Standards and Technology, nor is it intended to imply that the entities, materials, or equipment are necessarily the best available for the purpose.

Publication History

Approved by the NIST Editorial Review Board on 2023-01-25

How to Cite this NIST Technical Series Publication

Brown CU, Vogl GV, Tam WC (2023) Measuring Water Flow Rate for a Fire Hose Using a Wireless Sensor Network for Smart Fire Fighting: An Update Using Various Hose Conditions. (National Institute of Standards and Technology, Gaithersburg, MD), NIST Technical Note (TN) NIST TN 2245. <https://doi.org/10.6028/NIST.TN.2245>

NIST Author ORCID iDs

Christopher U. Brown: 0000-0002-0426-2249

Gregory W. Vogl: 0000-0003-4238-851X

Wai Cheong Tam: 0000-0003-3913-0243

Contact Information

christopher.brown@nist.gov

Abstract

A wireless sensor network was created to measure water-flow rate in a fire hose. An integrated electronic piezoelectric (IEPE) accelerometer was chosen as the sensor to measure the flow rate based on the vibrations generated by water flowing through a fire hose. The improved flow apparatus, including the accelerometer, was lightweight, small, and easily attached and removed to any location along the fire hose, not obstructing the water's flow path. The wireless flow apparatus was used with realistic firefighting hose conditions (i.e., holding the hose nozzle, nozzle motion during simulated fire suppression, simulated hose dragging) to evaluate the upgraded apparatus function and determine the influence of the hose motion, accelerometer location, and nozzle spray on the dominant-frequency metric. While more research is needed, such as enhancing the robustness of the dominant frequency metric, the preliminary research and this update shows the potential of a "smart" fire hose for improved situational awareness during fire suppression.

Keywords

Accelerometers; dominant frequency; fire hose; fire suppression; flow induced vibration; flow rate; hose vibration; sensors; smart firefighting; water flow rate measurement; wireless sensor network.

Table of Contents

1. Introduction	1
1.1. Goals	1
1.2. Brief Summary of Past Work.....	1
2. Updated Experimental Methods	2
2.1. Upgraded Hardware Attachment.....	2
2.2. Upgraded Accelerometer	3
2.3. Hose Conditions	3
2.3.1. Stationary – Hose on Ground	3
2.3.2. Stationary – Holding	5
2.3.3. Motion – Moving Nozzle in T-Pattern.....	6
2.3.4. Motion – Moving Hose Forward and Backward	6
2.3.5. Motion – Moving Hose Left and Right.....	7
2.4. Test Matrix.....	8
2.5. Data Collection Settings.....	8
2.6. Time-Domain to Frequency-Domain	9
3. Results and Discussion	9
3.1. Sensor at Front Hose Location – Stationary on Ground, Stationary Holding, and T-Pattern.....	9
3.2. Sensor at the Middle Hose Location – Stationary on Ground, Dragging, Moving Left and Right.....	16
3.3. Sensor at the Back Hose Location – Stationary on Ground, Dragging, Moving Left and Right	22
4. Uncertainty	25
5. Conclusions	26
6. Future Work	27
References	27

List of Tables

Table 1. The number of experiments conducted for the various hose conditions. 8

List of Figures

Fig. 1. The previous accelerometer (left) with base epoxied to the exterior hose fabric, and (right) the removable accelerometer strapped to the fire hose exterior. 2

Fig. 2. The sensor unit included the aluminum base, accelerometer, and protective plastic cover. The accelerometer was epoxied to an aluminum base under a plastic protective cover. A Velcro strap secured the sensor unit to the fire hose exterior. 2

Fig. 3. The hose nozzle set the hose stream to either a straight stream or a fog stream, while the bale on the nozzle changed the water flow rate. The commercial inline turbine flow meter measured the actual flow rate. 3

Fig. 4. The accelerometer at the front hose location for the hose in the stationary on ground condition, where the accelerometer was attached to the hose resting on concrete. The nozzle was elevated by the block to prevent vibrations between the nozzle and concrete. 4

Fig. 5. The accelerometer at the middle hose location for the hose in the stationary position where the accelerometer was attached to the hose resting on grass. 4

Fig. 6. The accelerometer at the back hose location for the hose in the stationary position where the accelerometer was attached to the hose resting on concrete. 5

Fig. 7. The accelerometer was elevated off the ground at the front hose location in the stationary holding position. The accelerometer was suspended between two blocks simulating the hose condition where the hose nozzle and hose were held off the ground. 5

Fig. 8. The accelerometer was elevated off the ground at the front hose location with the accelerometer either suspended between two blocks or held. The hose was moved in a T-pattern to simulate the lead firefighter directing water on a room fire with a backup firefighter supporting the hose. 6

Fig. 9. The accelerometer in the middle (left) and back (right) hose location on the ground was moved in line with the water flow direction to simulate the hose being dragged on the ground... 7

Fig. 10. The accelerometer in the middle (left) and back (right) hose location on the ground was moved left and right, perpendicular to the flow direction to simulate the hose being moved or dragged on the ground. 7

Fig. 11. An example of the raw acceleration data from a data burst (left), and the dominant frequency (circled) determined after the data was converted to the frequency-domain using a FFT (right). 9

Fig. 12. The dominant frequency for each flow rate with the accelerometer at the front hose location while the hose was stationary on the ground with a straight stream. 10

Fig. 13. The dominant frequency for each flow rate with the accelerometer at the front hose location while the hose was stationary on the ground with a fog stream. 10

Fig. 14. The dominant frequency for each flow rate with the accelerometer at the front hose location while the hose was held with a straight stream. 11

Fig. 15. The dominant frequency for each flow rate with the accelerometer at the front hose location while the hose was held with a fog stream. 12

Fig. 16. The dominant frequency for each flow rate with the accelerometer at the front hose location while the hose was moved in a T-pattern with a straight stream. 13

Fig. 17. The dominant frequency for each flow rate with the accelerometer at the front hose location while the hose was moved in a T-pattern with a fog stream. 13

Fig. 18. The dominant frequency for each flow rate with the accelerometer at the front hose location for all straight and fog stream experiments. 14

Fig. 19. The dominant frequency for each flow rate with the accelerometer at the front hose location for all straight stream experiments.15

Fig. 20. The dominant frequency for each flow rate with the accelerometer at the front hose location for all fog stream experiments.16

Fig. 21. The dominant frequency for each flow rate with the accelerometer at the middle hose location while the hose was stationary on the ground with a straight stream.17

Fig. 22. The dominant frequency for each flow rate with the accelerometer at the middle hose location while the hose was stationary on the ground with a fog stream.17

Fig. 23. The dominant frequency for each flow rate with the accelerometer at the middle hose location while the hose was moved to simulate dragging on the ground with a straight stream. 18

Fig. 24. The dominant frequency for each flow rate with the accelerometer at the middle hose location while the hose was moved to simulate dragging on the ground with a fog stream.18

Fig. 25. The dominant frequency for each flow rate with the accelerometer at the middle hose location while the hose was moved left and right on the ground with a straight stream.19

Fig. 26. The dominant frequency for each flow rate with the accelerometer at the middle location while the hose was moved left and right on the ground with a fog stream.19

Fig. 27. The dominant frequency for each flow rate with the accelerometer at the middle hose location for all straight and fog stream experiments.20

Fig. 28. The dominant frequency for each flow rate with the accelerometer at the middle location for all straight stream experiments.21

Fig. 29. The dominant frequency for each flow rate with the accelerometer at the middle location for all fog stream experiments.21

Fig. 30. The dominant frequency for each flow rate with the accelerometer at the back hose location while the hose was stationary on the ground with a straight stream.22

Fig. 31. The dominant frequency for each flow rate with the accelerometer at the back hose location while the hose was stationary on the ground with a fog stream.23

Fig. 32. The dominant frequency for each flow rate with the accelerometer at the back hose location while the hose was moved to simulate dragging on the ground with a straight stream. 23

Fig. 33. The dominant frequency for each flow rate with the accelerometer at the back hose location while the hose was moved to simulate dragging on the ground with a fog stream.24

Fig. 34. The dominant frequency for each flow rate with the accelerometer at the back hose location while the hose was moved left and right on the ground with a straight stream.24

Fig. 35. The dominant frequency for each flow rate with the accelerometer at the back hose location while the hose was moved left and right on the ground with a fog stream.25

1. Introduction

1.1. Goals

The overall goal of these experiments is to develop a robust, wireless, flow apparatus:

1. to measure water flow through a fire hose or fire suppression water pipe
2. that is portable, small, and durable
3. that has a flexible, easy, external attachment at any location along a fire hose or pipe
4. for the incident commander to easily determine water flow via a portable electronic device

Such a device would improve firefighting situational awareness and provide additional information for an incident commander to determine which fire hoses are supplying water, and how much, at a complex incident scene.

The goal of this report is to provide an update on experiments that have occurred since the previous reports [1-4] and to outline future work. This report explores:

1. how the wireless flow apparatus functions under realistic firefighting hose movements (holding the hose nozzle, nozzle motion during simulated fire suppression, hose motion during simulated hose dragging)
2. if the system responds differently at different locations along a fire hose (front, middle, back)
3. if the system is affected by the type of nozzle stream (straight stream versus a fog stream)

1.2. Brief Summary of Past Work

This Technical Note is an update and an extension of previous research conducted at the National Institute of Standards and Technology (NIST) as part of the Smart Firefighting Project. During the first phase of this project, a wired flow apparatus was developed with a wired accelerometer epoxied to the exterior fabric of a flexible fire hose that detected water flow vibrations [1,3]. Two metrics were assessed to determine flow rate. The first metric examined was the standard deviation of acceleration of hose vibrations. This metric displayed a consistent, inverted, bell-shaped curve with increasing flow rate and was not ideal. The second metric was the dominant frequency of the hose vibrations, which decreased with increasing flow rate, a relationship typically found with flow in rigid pipes. A single hose condition, the hose stationary on the ground, was used throughout those experiments.

The next phase involved developing a wireless sensor network using an accelerometer epoxied to the exterior fabric of a flexible fire hose and the dominant frequency metric [2,4]. A single hose condition, the hose stationary on the ground, was used throughout those experiments. The dominant frequency decreased with increasing flow rate, but the metric was not as robust, and the overall dominant frequency shifted depending on the position of the hose on the ground. A

graphical user interface (GUI) dashboard displayed the general flow conditions in real-time to an incident commander.

2. Updated Experimental Methods

2.1. Upgraded Hardware Attachment

Previously the accelerometer base was epoxied to the outer surface of the hose which limited the position of the accelerometer along the hose [Fig. 1]. For these current experiments, the accelerometer was epoxied to an aluminum alloy base to provide more flexibility with the accelerometer location on the hose. The aluminum base was strapped tightly with Velcro to the hose [Fig. 2]. The accelerometer was protected with a plastic cover attached to the aluminum base. The removable sensor unit (aluminum base, accelerometer, and plastic protective cover) offered flexibility to attach and remove the accelerometer anywhere along the hose.

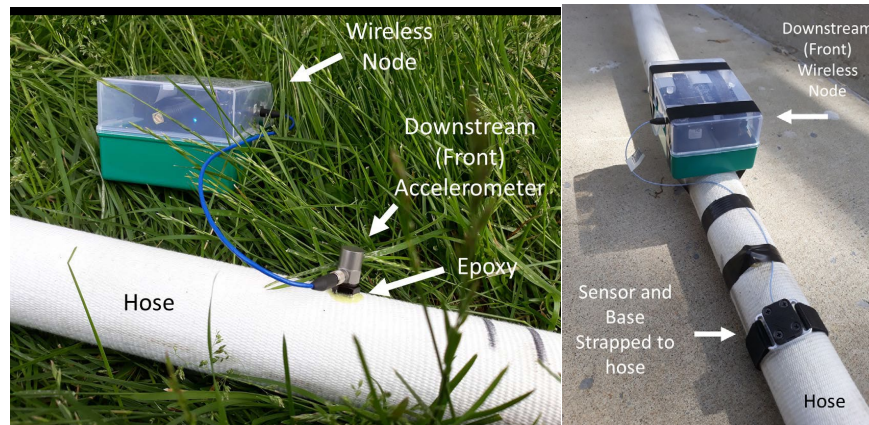


Fig. 1. The previous accelerometer (left) with base epoxied to the exterior hose fabric, and (right) the removable accelerometer strapped to the fire hose exterior.

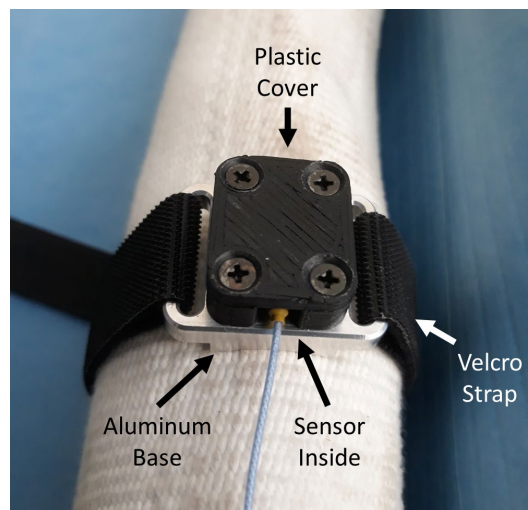


Fig. 2. The sensor unit included the aluminum base, accelerometer, and protective plastic cover. The accelerometer was epoxied to an aluminum base under a plastic protective cover. A Velcro strap secured the sensor unit to the fire hose exterior.

2.2. Upgraded Accelerometer

Previously, a larger accelerometer (PCB Piezotronics 352C33) was used to collect the vibration data. For these experiments, a smaller accelerometer (PCB Piezotronics 352A24) was applied to reduce weight and reduce the size of the accelerometer for practical field application. The profile of the sensor unit including the protective plastic cover was therefore reduced.

2.3. Hose Conditions

The same commercial fire-suppression hose with nominal 4.5 cm (1.75 in) inner diameter, and approximately 15 m (50 ft) long, was used as described in previous experiments [1]. The sensor unit was strapped to three different hose locations: front, middle, and back. The front location was approximately 2.4 m (8 ft) from the hose nozzle. The middle location was approximately the middle of the hose length, or 7.6 m (25 ft) from the hose nozzle. The back location was approximately 2.4 m (8 ft) from the upstream hose attachment point to the water source. A typical fog-style hose nozzle was used to set either a straight stream or fog stream as well as to change the flow rate. A commercial turbine flow meter was attached between the nozzle and the fire hose to measure the actual water flow rate [Fig. 3].

Previous experiments were conducted with the hose in a stationary position on the grass and concrete in a straight stream configuration. For these current experiments, data was collected with the nozzle set for a straight stream or a fog stream for several hose conditions: hose stationary on and above the ground, hose nozzle motion simulating fire suppression, and hose motion on the ground simulating dragging.

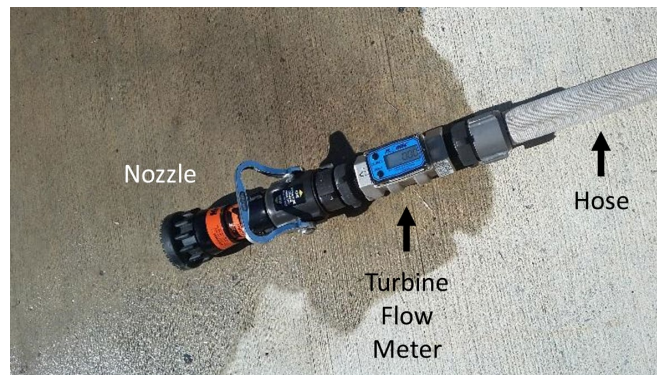


Fig. 3. The hose nozzle set the hose stream to either a straight stream or a fog stream, while the bale on the nozzle changed the water flow rate. The commercial inline turbine flow meter measured the actual flow rate.

2.3.1. Stationary – Hose on Ground

For the stationary hose condition on the ground, the accelerometer was positioned at the front, middle, and back locations [Fig 4-6]. The accelerometer at the front and back hose locations was attached to the hose on concrete, while the hose was on grass at the middle hose location. The nozzle was elevated by a cinder block, hanging off and not contacting the block, to prevent impacts between the nozzle and concrete that might have been detected by the accelerometer.

For this hose condition, the water flow vibrations detected by the accelerometer may be affected by the ground, either concrete or grass. This hose configuration simulated a firefighter holding the hose nozzle while the remaining hose including the accelerometer was on the ground.



Fig. 4. The accelerometer at the front hose location for the hose in the stationary on ground condition, where the accelerometer was attached to the hose resting on concrete. The nozzle was elevated by the block to prevent vibrations between the nozzle and concrete.

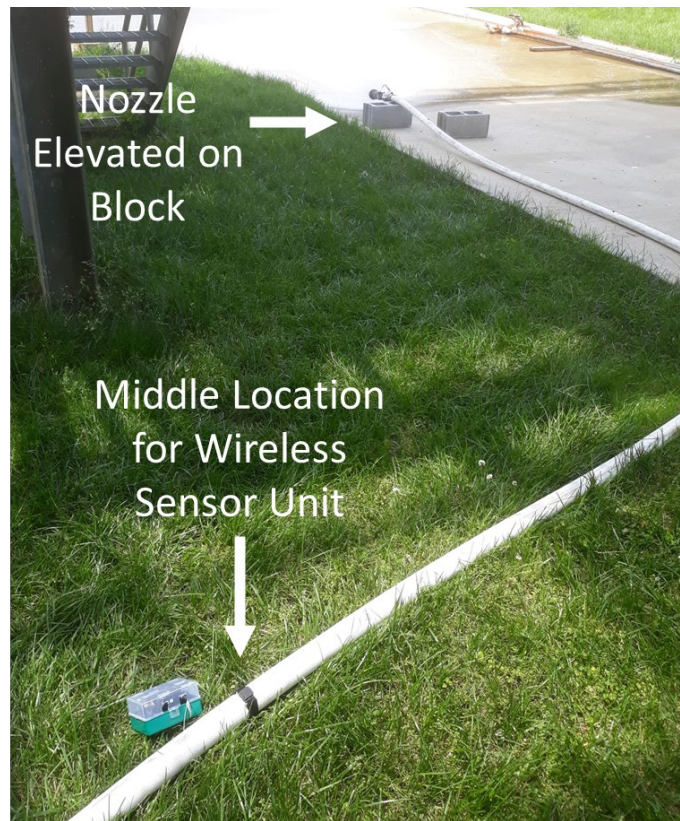


Fig. 5. The accelerometer at the middle hose location for the hose in the stationary position where the accelerometer was attached to the hose resting on grass.



Fig. 6. The accelerometer at the back hose location for the hose in the stationary position where the accelerometer was attached to the hose resting on concrete.

2.3.2. Stationary – Holding

For the hose condition where the hose was held stationary, the accelerometer was only attached at the front hose location. The hose and nozzle were elevated off the ground, either held by a person, or the sensor was suspended between cinder blocks to simulate a person holding the hose and nozzle [Fig. 7]. When the nozzle was suspended on blocks, the nozzle was elevated above the concrete to reduce water flow vibrations between the nozzle and concrete that might be detected by the accelerometer. For this hose condition, the water flow vibrations should not be affected by the ground, as in the stationary hose on ground condition [Fig. 4].



Fig. 7. The accelerometer was elevated off the ground at the front hose location in the stationary holding position. The accelerometer was suspended between two blocks simulating the hose condition where the hose nozzle and hose were held off the ground.

2.3.3. Motion – Moving Nozzle in T-Pattern

For this condition, the accelerometer was in the front location, elevated off the ground, with the nozzle held by a person, and a second person holding the hose upstream of the sensor such that the sensor was suspended between holding points. In most cases, the hose was supported by two blocks with the sensor suspended between the blocks to simulate two people holding the hose. For either case, the hose nozzle was moved in a T-pattern to simulate the lead firefighter directing water on a room fire with a backup firefighter supporting the hose [Fig. 8]. The nozzle was elevated above the concrete to reduce water flow vibrations between the nozzle and concrete that might be detected by the accelerometer. Motion of the hose was maintained during the data acquisition phase for the accelerometer. This hose condition added motion to the previous hose holding condition [Fig. 7] by introducing only the effect of the hose motion to the water flow vibrations.

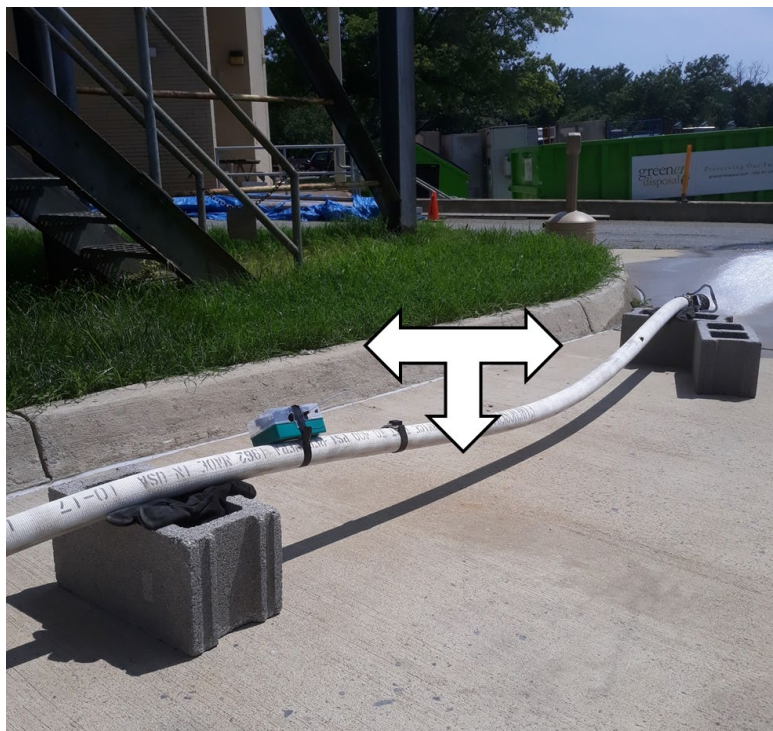


Fig. 8. The accelerometer was elevated off the ground at the front hose location with the accelerometer either suspended between two blocks or held. The hose was moved in a T-pattern to simulate the lead firefighter directing water on a room fire with a backup firefighter supporting the hose.

2.3.4. Motion – Moving Hose Forward and Backward

For this condition, the accelerometer was in either the middle or back hose location, with the accelerometer attached to the hose resting on the grass or concrete. The hose was moved forward and backward in line with the flow direction to simulate the hose being dragged on the ground [Fig. 9]. Motion of the hose was maintained during each data acquisition phase for the accelerometer for approximately 1 s. This hose condition was similar to the stationary hose on ground condition [Fig. 5-6] but with the additional hose motion that may affect the vibrations detected by the accelerometer.

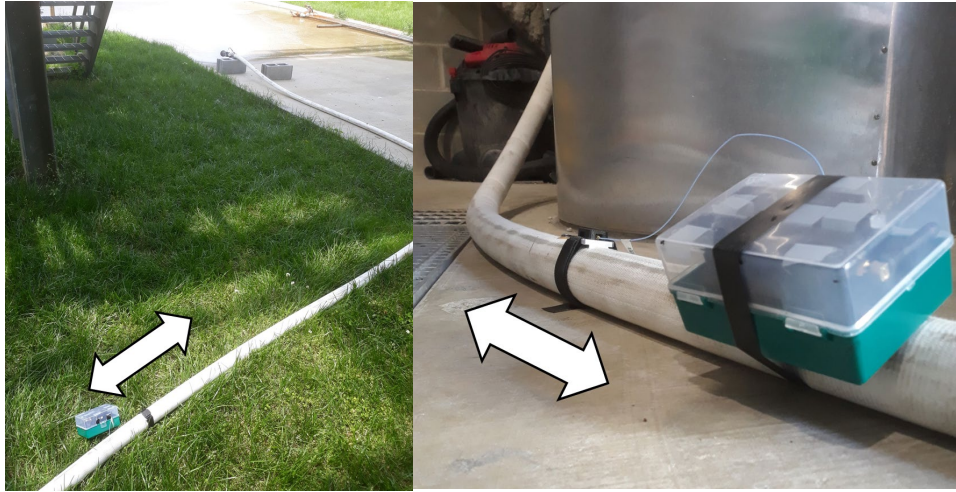


Fig. 9. The accelerometer in the middle (left) and back (right) hose location on the ground was moved in line with the water flow direction to simulate the hose being dragged on the ground.

2.3.5. Motion – Moving Hose Left and Right

For this condition, the accelerometer was in either the middle or back hose location, with the accelerometer attached to the hose resting on the grass or concrete. The hose was moved left and right, perpendicular to the flow direction, to simulate the hose being moved or dragged on the ground [Fig. 10]. The left and right motion of the hose at various frequencies was maintained during the data acquisition phase for the accelerometer. This hose condition was similar to the forward and backward hose movement [Fig 9] but the motion was perpendicular to the water flow direction.

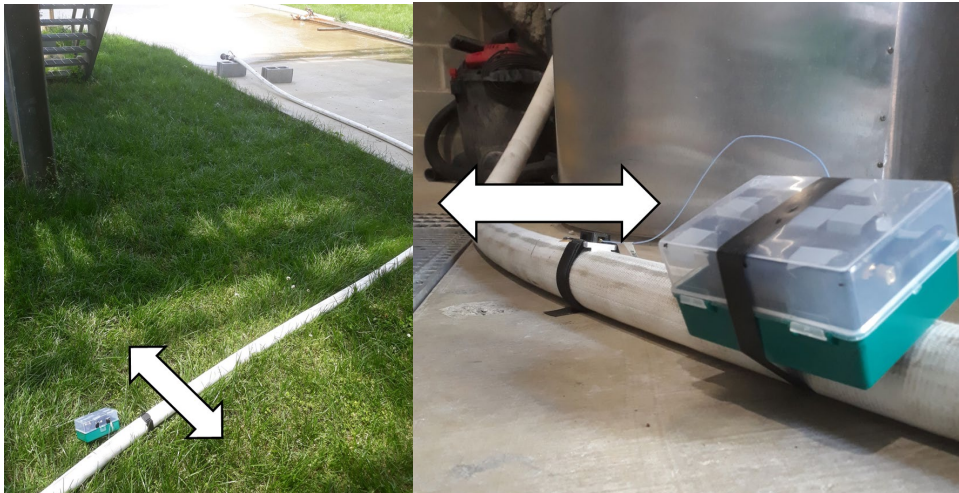


Fig. 10. The accelerometer in the middle (left) and back (right) hose location on the ground was moved left and right, perpendicular to the flow direction to simulate the hose being moved or dragged on the ground.

2.4. Test Matrix

The following table summarizes the number of experiments for each hose location, nozzle stream, and hose condition [Tab. 1].

Table 1. The number of experiments conducted for the various hose conditions.

Accelerometer Location on Hose	Nozzle Stream	Hose Condition	Number of Experiments
Front	Straight	Stationary - On ground	6
	Fog	Stationary - On ground	5
	Straight	Stationary - Holding	13
	Fog	Stationary - Holding	11
	Straight	Motion – T-Pattern	6
	Fog	Motion – T-Pattern	4
Middle	Straight	Stationary - On ground	4
	Fog	Stationary - On ground	3
	Straight	Motion – Left / Right	5
	Fog	Motion – Left / Right	3
	Straight	Motion - Dragging	3
	Fog	Motion - Dragging	3
Back	Straight	Stationary - On ground	4
	Fog	Stationary - On ground	4
	Straight	Motion – Left / Right	3
	Fog	Motion – Left / Right	3
	Straight	Motion - Dragging	3
	Fog	Motion - Dragging	3

2.5. Data Collection Settings

Besides the hose conditions, several other experimental parameters were modified compared to the previously documented experiments [1-4]. The approximate flow rates used for these current experiments ranged from 0 LPM to approximately 568 LPM (150 GPM), in increments of approximately 114 LPM (30 GPM), instead of increments of 19 LPM (5 GPM) as was done previously (the abbreviation ‘LPM’ represents liters per minute and ‘GPM’ represents gallons per minute for the remaining text). The fewer number of flow rates helped streamline the experiments. In the future, if more flow rate data are needed, then more flow rates will be applied.

The wireless sensor network transmits data from the accelerometer to the laptop computer’s base station in synchronized bursts. During the data sampling phase, the accelerometer measures the vibration data and then the wireless node transmits that data to the laptop computer’s base station during the transmission phase. Generally, when the burst duration is shorter, the transmissions can occur more frequently.

In the previous set of experiments, two, data-collection arrangements were used. First, a sampling frequency of 10 kHz with a data burst of 0.19 s was initially used. Second, a sampling frequency of 1 kHz with a data burst of 10 s was used in order to collect larger amounts of data and reduce dominant frequency data scatter.

For these current experiments, one data-collection arrangement was used, a 10 kHz sampling frequency with a 1 s burst of data every 30 seconds. Initially 5 bursts of data were collected at each flow rate, but this was increased to 10 bursts to be able to discard outliers in the data and still have 5 data bursts.

2.6. Time-Domain to Frequency-Domain

As described previously, the time-domain, acceleration data collected from the accelerometers [Fig. 11] from the 10 data bursts were converted to the frequency-domain using a Fast Fourier Transform (FFT) [1-4] [Fig. 11] and an average dominant frequency at each flow rate was calculated. A decreasing trend for dominant frequency was noted in the previous studies with increasing flow rate.

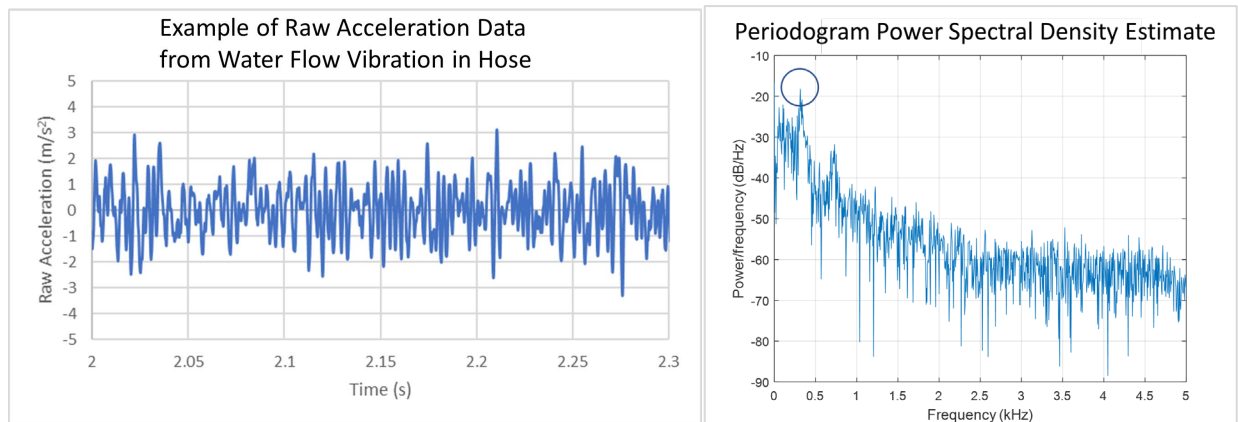


Fig. 11. An example of the raw acceleration data from a data burst (left), and the dominant frequency (circled) determined after the data was converted to the frequency-domain using a FFT (right).

3. Results and Discussion

3.1. Sensor at Front Hose Location – Stationary on Ground, Stationary Holding, and T-Pattern

The accelerometer was strapped at the front hose location approximately 2.4 m (8 ft) from the hose nozzle that was elevated off the ground to reduce water flow vibrations between the nozzle and ground that might be detected by the accelerometer.

For the stationary, hose on-ground condition, there were 6 experiments with the straight stream [Fig. 12] and 5 experiments with the fog stream [Fig. 13]. Each experiment included five (5), 1 s, data collection bursts for a total of 30 dominant frequencies for each flow rate for the straight stream and 25 dominant frequencies for each flow rate for the fog stream. The following figures include ‘Box and Whisker’ graphs. Each candle bar at a single flow rate represents the population of either 30 dominant frequency data points for straight-stream experiments or 25 dominant frequency data points for fog-stream experiments. The solid line across the bar represents the median and the bar range is determined from the 1st and 3rd quartile. An individual

dot represents an outlier as determined by the graphing software algorithm. The ‘x’ within each bar is the mean dominant frequency for each flow rate including outliers.

Neither the straight stream nor the fog stream had decreasing dominant frequencies with increasing flow rate as expected based on previous results. A unique dominant frequency was not observed for each flow rate. Both the fog stream and straight stream data showed similar variability.

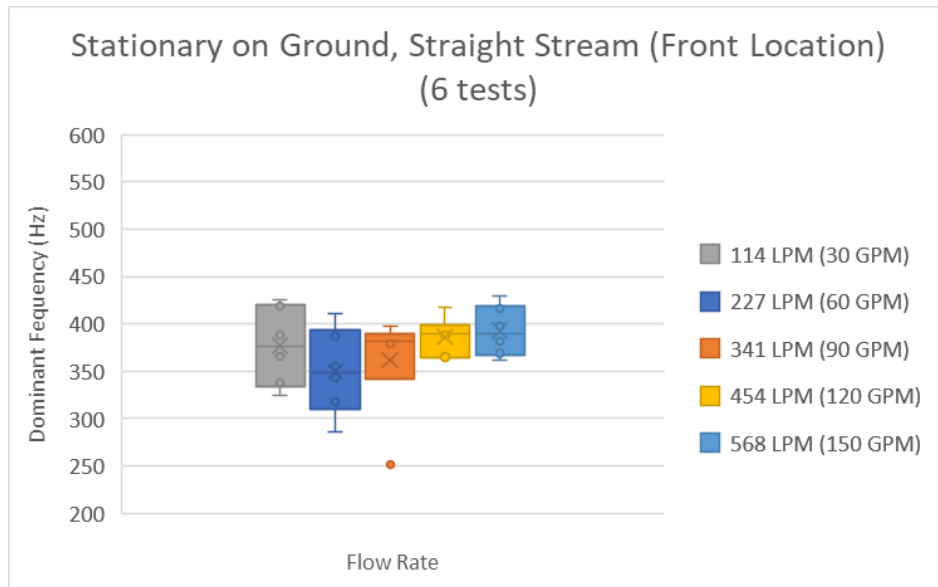


Fig. 12. The dominant frequency for each flow rate with the accelerometer at the front hose location while the hose was stationary on the ground with a straight stream.

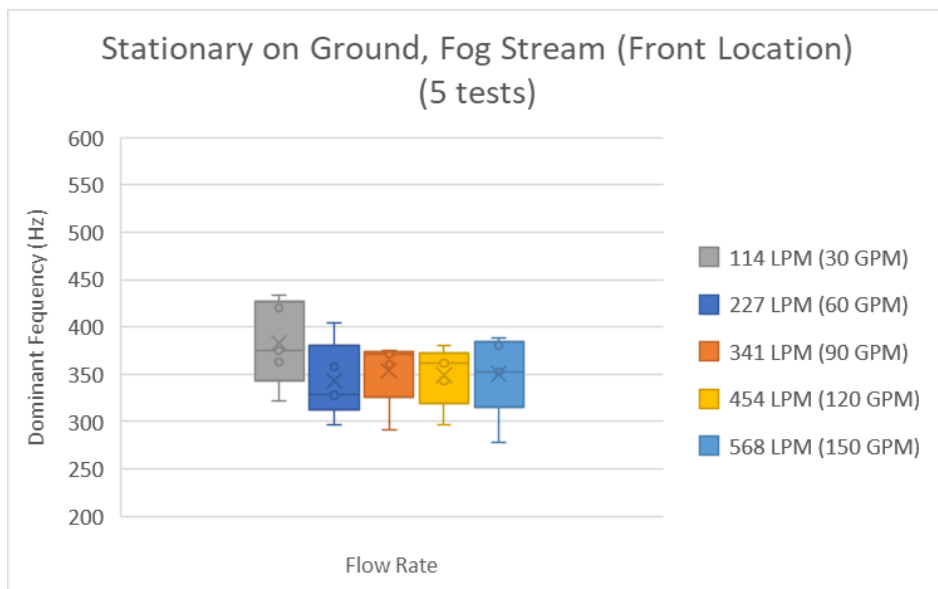


Fig. 13. The dominant frequency for each flow rate with the accelerometer at the front hose location while the hose was stationary on the ground with a fog stream.

For the stationary, hose-holding condition, there were 13 experiments with the straight stream [Fig. 14] and 11 experiments with the fog stream [Fig. 15]. Each experiment included five (5), 1 s, data collection bursts for a total of 65 dominant frequencies for each flow rate for the straight stream and 55 dominant frequencies for the fog stream. For the holding condition, the hose was either held by a person, or suspended between two blocks, so the accelerometer was suspended off the ground to simulate the nozzle being held by a firefighter. Depending on the holding configuration, the accelerometer was either approximately 1 m (3 ft) (person holding) or approximately 2.4 m (8 ft) (when suspended) from the hose nozzle.

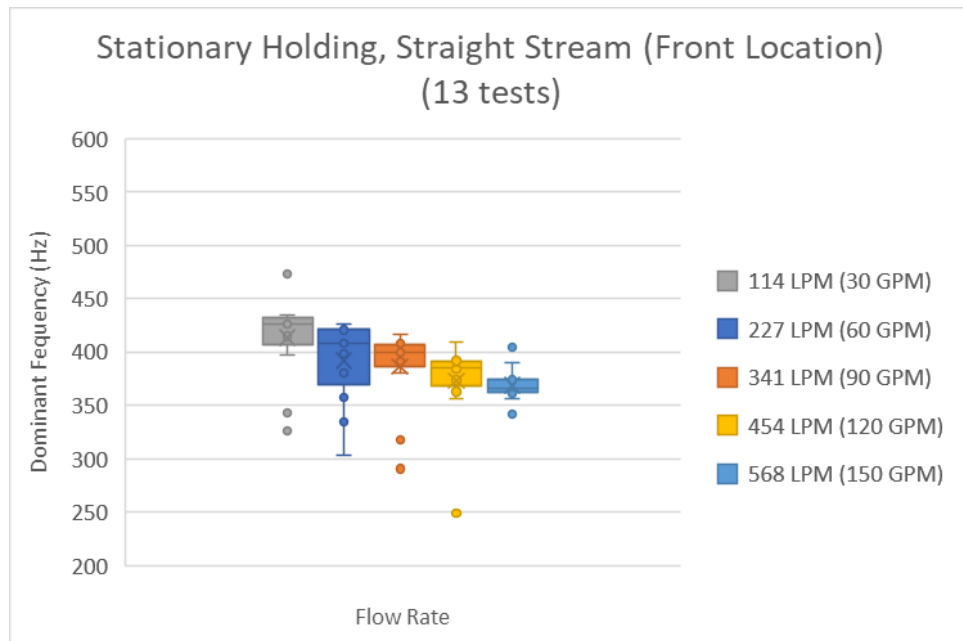


Fig. 14. The dominant frequency for each flow rate with the accelerometer at the front hose location while the hose was held with a straight stream.

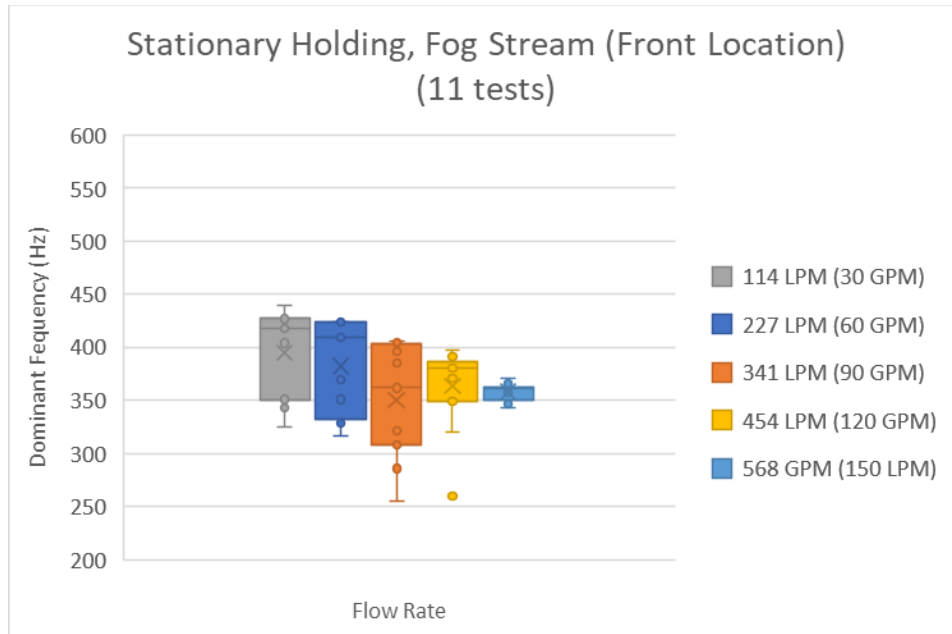


Fig. 15. The dominant frequency for each flow rate with the accelerometer at the front hose location while the hose was held with a fog stream.

Both the straight and fog stream experiments showed trends towards a decreasing dominant frequency with increasing flow rate, however because of the variability of the data from one flow rate to the next, there was not a unique dominant frequency for each flow rate. The fog stream data showed more variability than the straight stream data.

For the hose condition where the hose was moved in a T-pattern to simulate fire suppression, there were 6 experiments with the straight stream [Fig. 16] and 4 experiments with the fog stream [Fig. 17]. Each experiment included five (5), 1 s, data collection bursts for a total of 30 dominant frequencies for each flow rate for the straight stream and 20 dominant frequencies for each flow rate for the fog stream. The hose was either held by two people, or suspended between two blocks, so the sensor was suspended between each person while in motion, to simulate being held by two firefighters during fire suppression.

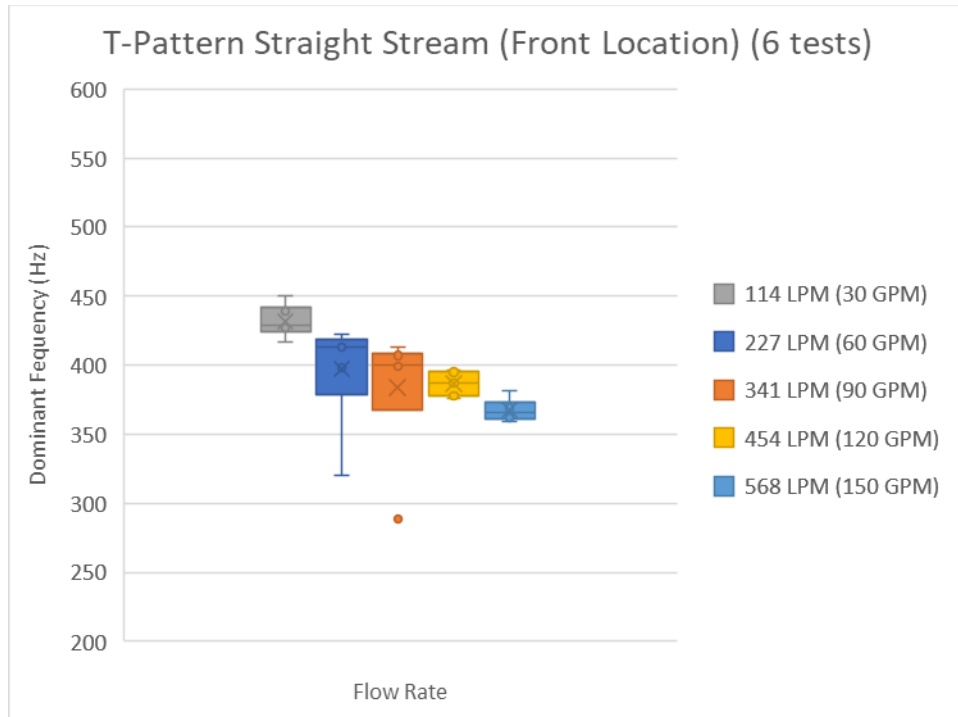


Fig. 16. The dominant frequency for each flow rate with the accelerometer at the front hose location while the hose was moved in a T-pattern with a straight stream.

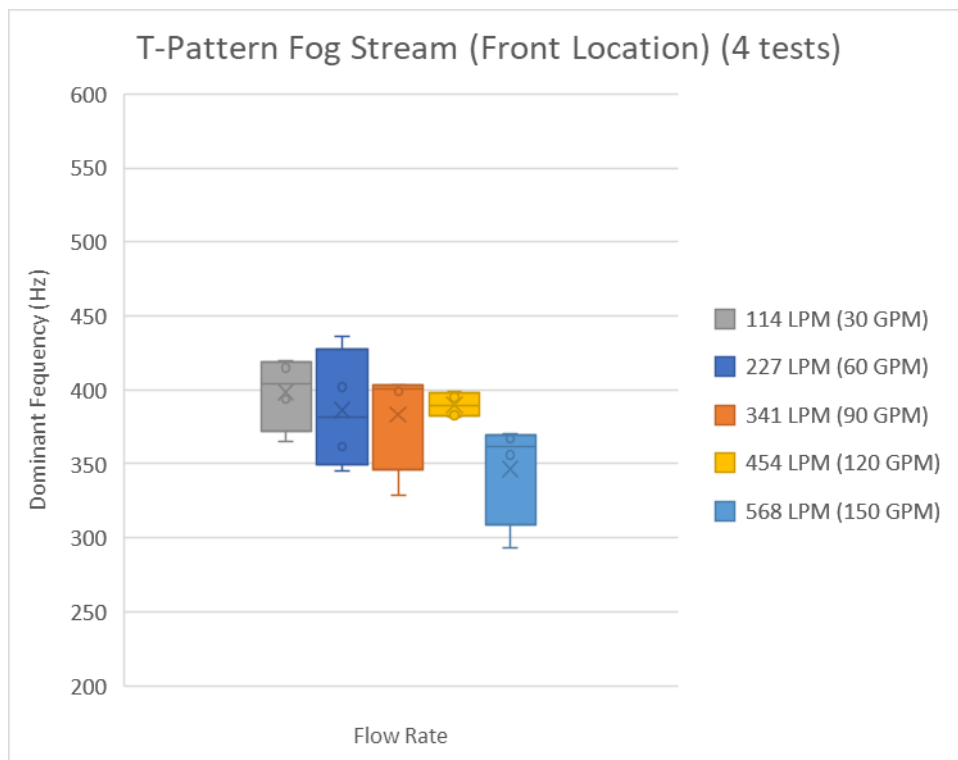


Fig. 17. The dominant frequency for each flow rate with the accelerometer at the front hose location while the hose was moved in a T-pattern with a fog stream.

Both the straight and fog stream experiments showed trends towards a decreasing dominant frequency with increasing flow rate, however based on the variability of the data from one flow rate to the next, there was not a unique dominant frequency for each flow rate. The fog stream data showed more variability than the straight stream data.

At the front hose location, the T-pattern condition, where the hose was in motion, was compared to the hose holding condition, where the hose was stationary. The similar results suggest that the low frequency, T-pattern, motion of the hose did not appear to affect the dominant frequency or data variability.

At the front location, the elevated hose in motion (T-pattern) and elevated hose while held, had less variability and a clearer decreasing trend than the hose resting on the ground. This suggests that having the accelerometer off the ground or in motion may dampen extreme vibrations or reduce variability in the vibration data. When the hose was stationary on the ground, the interaction between the hose and the ground may have influenced the vibrations.

Additional focus was applied to the data at the front hose location to further examine the response of the dominant frequency when all the hose conditions were combined into one graph [Fig. 18]. The average, dominant frequency values indicated a decreasing trend with flow rate but the variability in the data was high.

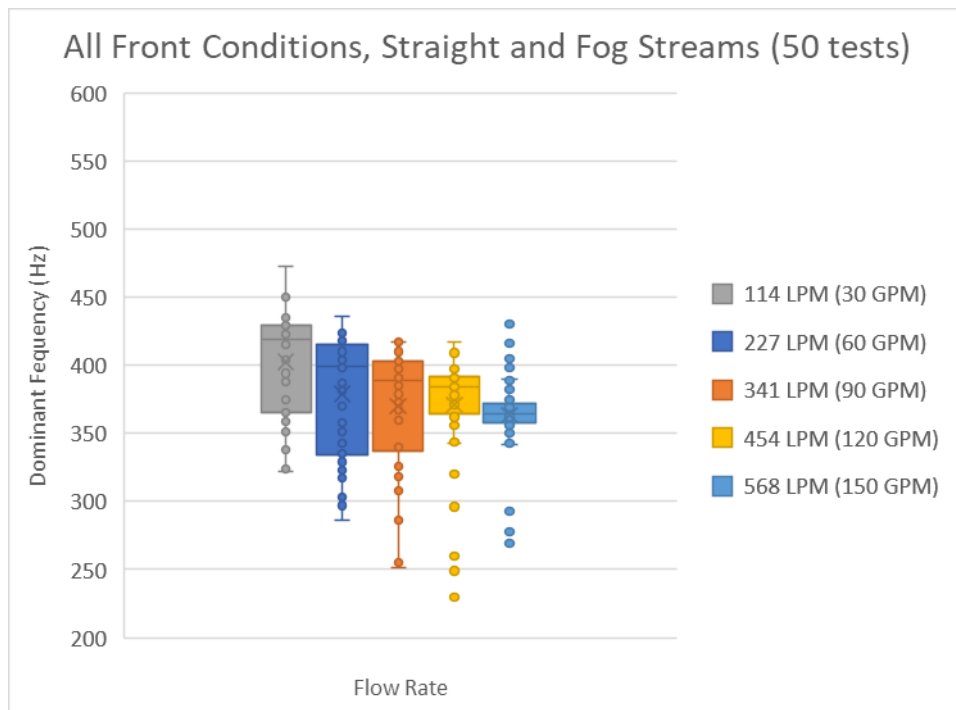


Fig. 18. The dominant frequency for each flow rate with the accelerometer at the front hose location for all straight and fog stream experiments.

The straight [Fig. 19] (28 experiments) and fog stream [Fig. 20] (22 experiments) data were then plotted separately to examine the effects of the stream type on the experiments. The hose nozzle

stream type, either straight stream or fog stream, did not appear to influence the dominant frequency. The decreasing trend of dominant frequency was clearer for the straight stream than for the fog stream, however due to the variability in the data for the straight stream, the decreasing trend did not correspond to a unique dominant frequency for each flow rate. If the fog nozzle stream generated additional vibrations, they may not be in the frequency range to affect the dominant frequency, or the vibrations may not be detectable upstream where the accelerometer was located. For future tests, a smooth bore nozzle will also be used.

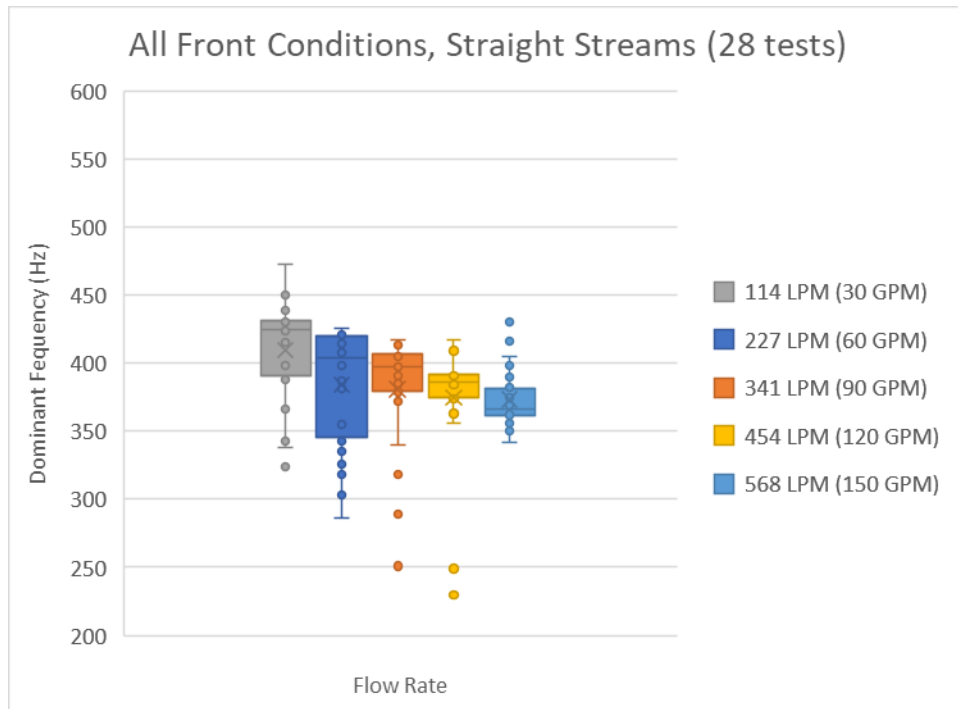


Fig. 19. The dominant frequency for each flow rate with the accelerometer at the front hose location for all straight stream experiments.

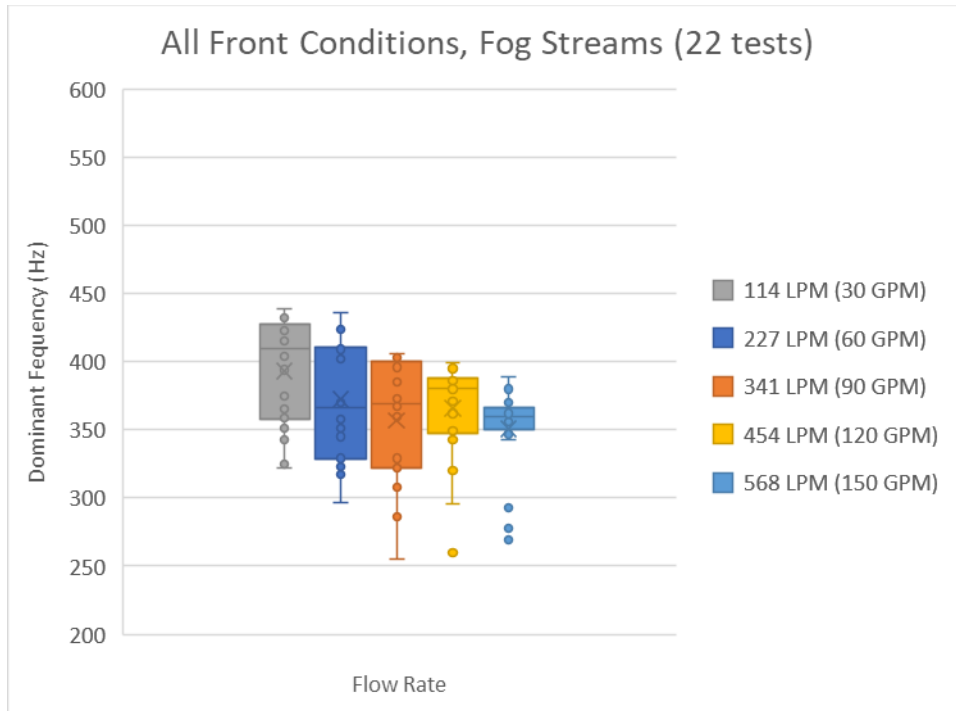


Fig. 20. The dominant frequency for each flow rate with the accelerometer at the front hose location for all fog stream experiments.

3.2. Sensor at the Middle Hose Location – Stationary on Ground, Dragging, Moving Left and Right

The accelerometer was attached to the middle hose location approximately 7.6 m (25 ft) from the hose nozzle where the hose rested on grass. The nozzle was elevated off the ground to reduce water flow vibrations between the nozzle and ground that might be detected by the accelerometer.

For the stationary, hose on-ground condition, there were 4 experiments with the straight stream [Fig. 21] and 3 experiments with the fog stream [Fig. 22]. Each experiment included five (5), 1 s, data collection bursts for a total of 20 dominant frequencies for each flow rate for the straight stream and 15 dominant frequencies for each flow rate for the fog stream. Neither the straight stream nor the fog stream had a unique dominant frequency for each flow rate. Both the fog stream and straight stream data showed similar variability.

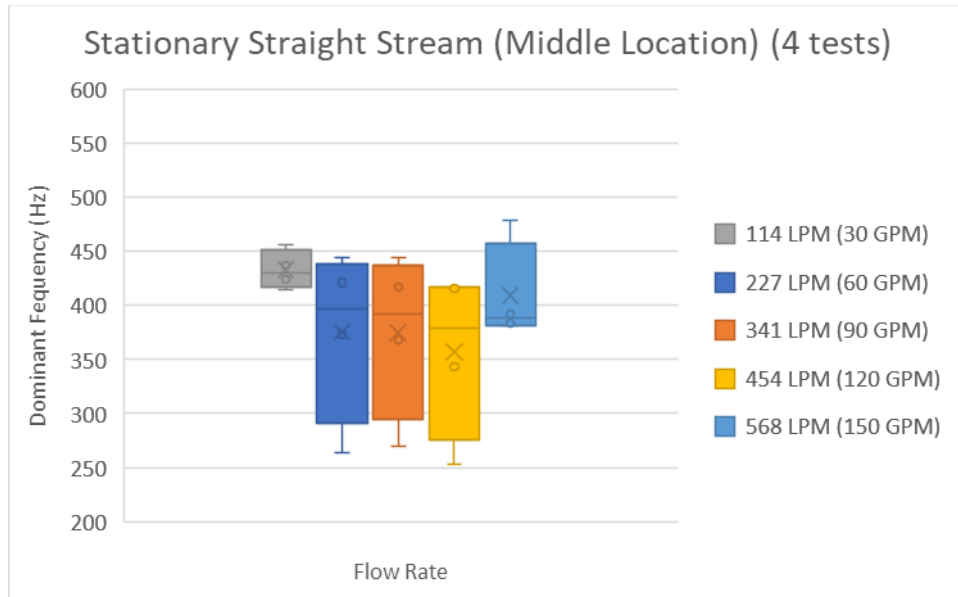


Fig. 21. The dominant frequency for each flow rate with the accelerometer at the middle hose location while the hose was stationary on the ground with a straight stream.

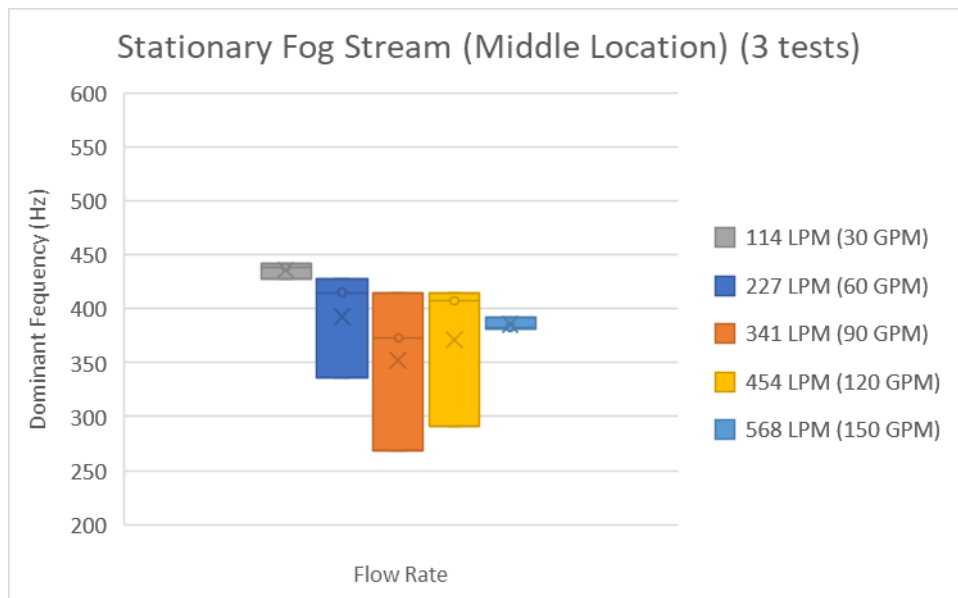


Fig. 22. The dominant frequency for each flow rate with the accelerometer at the middle hose location while the hose was stationary on the ground with a fog stream.

For the condition where the hose was moved forward and backward to simulate dragging, there were 3 experiments with the straight stream [Fig. 23] and 3 experiments with the fog stream [Fig. 24]. Each experiment included five (5), 1 s, data collection bursts for a total of 15 dominant frequencies for each flow rate for the straight stream and 15 dominant frequencies for each flow rate for the fog stream.

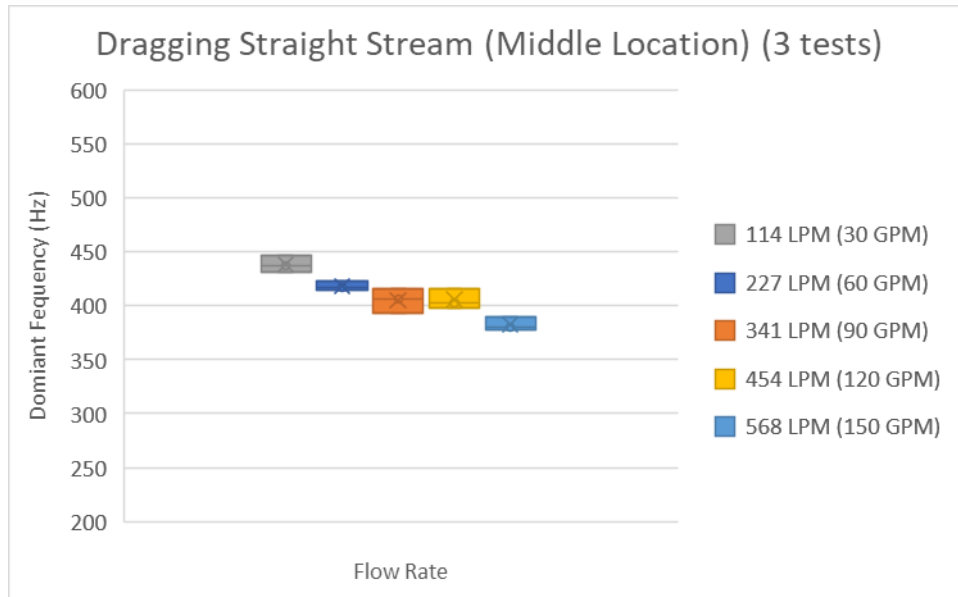


Fig. 23. The dominant frequency for each flow rate with the accelerometer at the middle hose location while the hose was moved to simulate dragging on the ground with a straight stream.

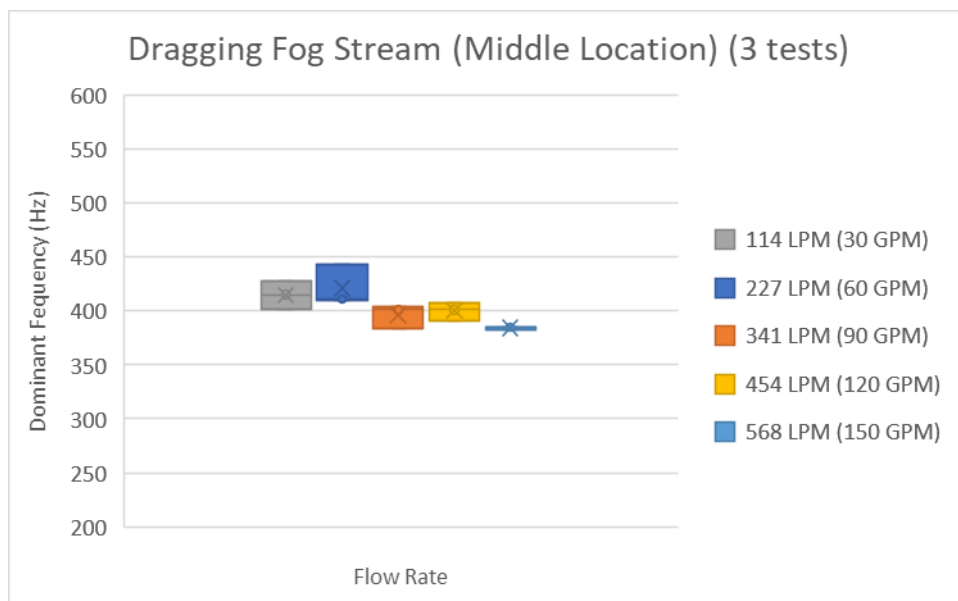


Fig. 24. The dominant frequency for each flow rate with the accelerometer at the middle hose location while the hose was moved to simulate dragging on the ground with a fog stream.

Both the straight and fog stream showed trends towards a decreasing dominant frequency with increasing flow rate, however based on the variability of the data from one flow rate to the next, there was not a unique dominant frequency for each flow rate. There was, however, less variability for both the fog stream and straight stream data compared to the other experiments.

For the condition where the hose was moved left and right compared to the water flow direction, there were 5 experiments with the straight stream [Fig. 25] and 3 experiments with the fog stream [Fig. 26]. Each experiment included five (5), 1 s, data collection bursts for a total of 25 dominant frequencies for each flow rate for the straight stream and 15 dominant frequencies for each flow rate for the fog stream. Both the straight and fog stream showed trends towards a decreasing dominant frequency with increasing flow rate, however based on the variability of the data from one flow rate to the next, there was not a unique dominant frequency for each flow rate.

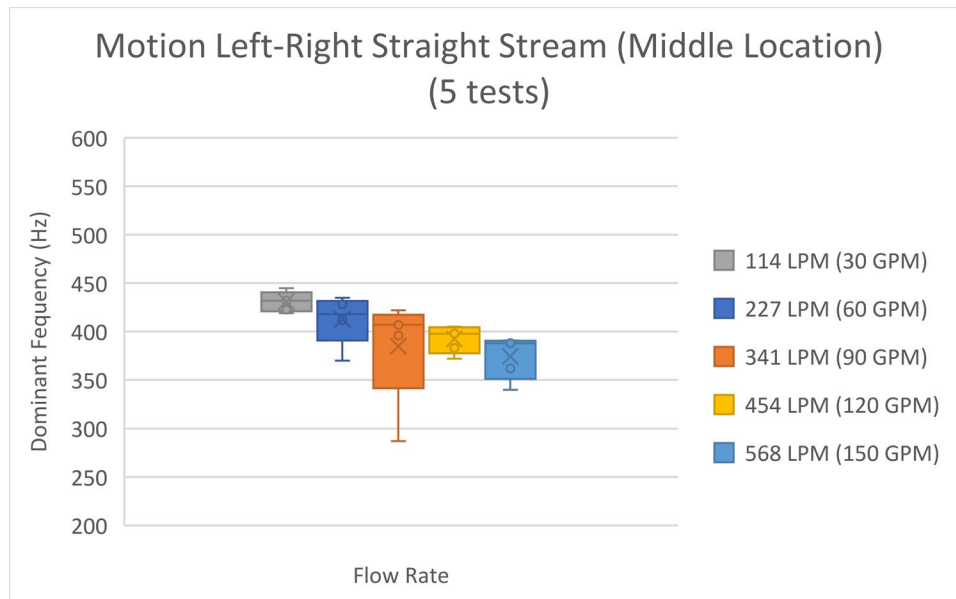


Fig. 25. The dominant frequency for each flow rate with the accelerometer at the middle hose location while the hose was moved left and right on the ground with a straight stream.

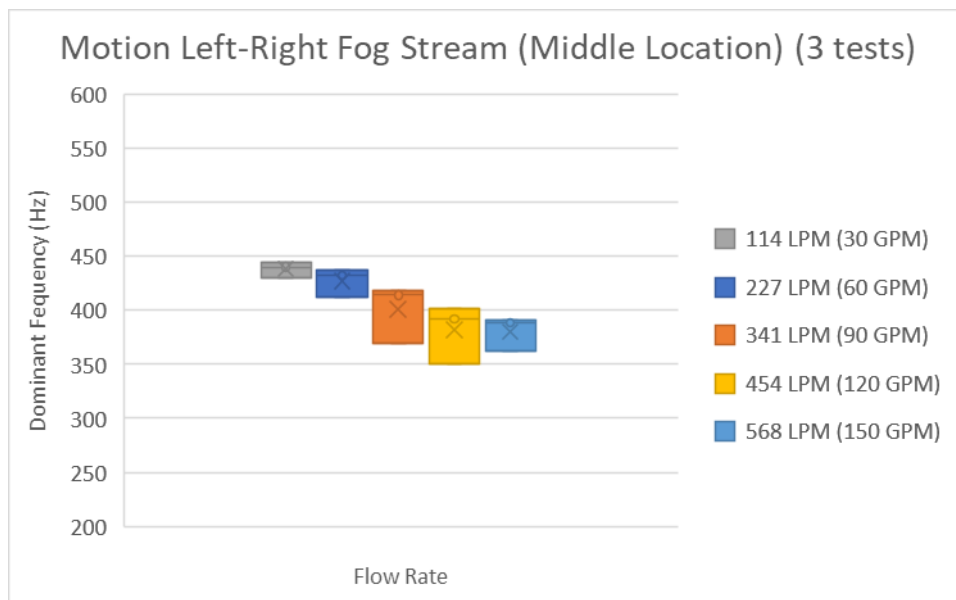


Fig. 26. The dominant frequency for each flow rate with the accelerometer at the middle location while the hose was moved left and right on the ground with a fog stream.

At the middle hose location, the motion of the hose in the direction of the flow (dragging) compared to the motion perpendicular to the flow (left-right) resulted in a similar dominant frequency response. The similar response suggests that the direction of hose motion while on the ground does not influence the dominant frequency.

At the middle hose location, the hose motion conditions (dragging and left-right) had less variability and a clearer decreasing trend compared to the stationary on-ground condition at this location. This suggests that the motion of the accelerometer may dampen extreme vibrations or reduce variability in the vibration data.

Additional focus was applied to the data at the middle hose location to further examine the response of the dominant frequency when all 21 experiments were combined into one plot [Fig. 27]. The average dominant frequency values indicate a decreasing trend with flow rate with less variability in the data than for the front location.

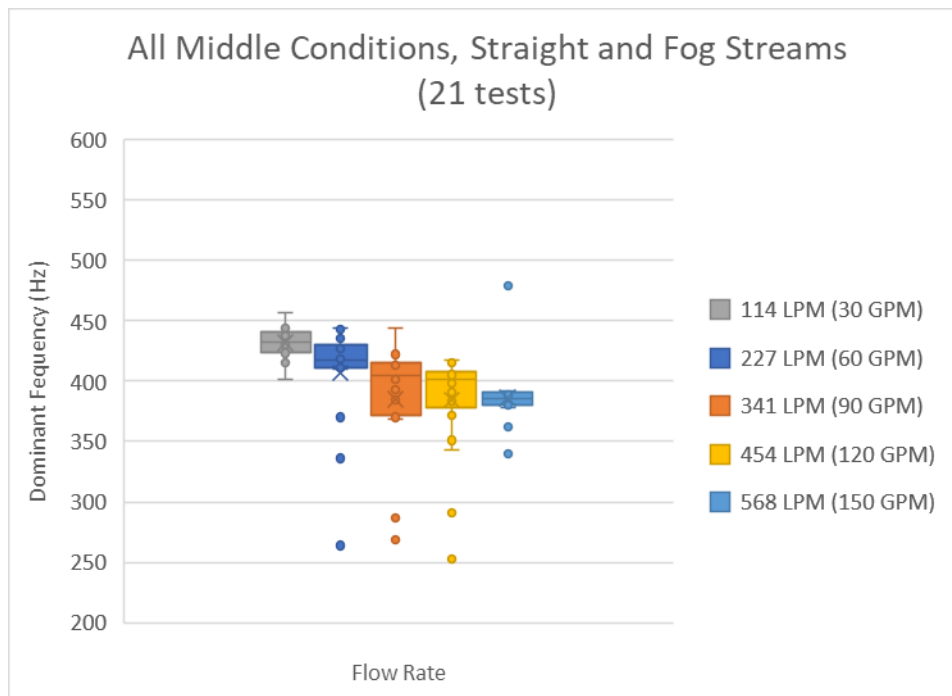


Fig. 27. The dominant frequency for each flow rate with the accelerometer at the middle hose location for all straight and fog stream experiments.

The straight [Fig. 28] (12 experiments) and fog [Fig. 29] (9 experiments) stream data were then plotted separately to examine the effects of the stream type on the experiments. At the middle hose location, similarly to the front hose location, the hose nozzle stream type, either straight stream or fog stream, did not appear to influence the dominant frequency. Both decreasing trends of dominant frequency were similar without a unique dominant frequency for each flow rate for the straight and fog stream experiments. If the fog nozzle stream creates vibrations, they may not be in the frequency range to affect the dominant frequency, or the vibrations may not be detectable upstream at the middle hose location where the accelerometer was located.

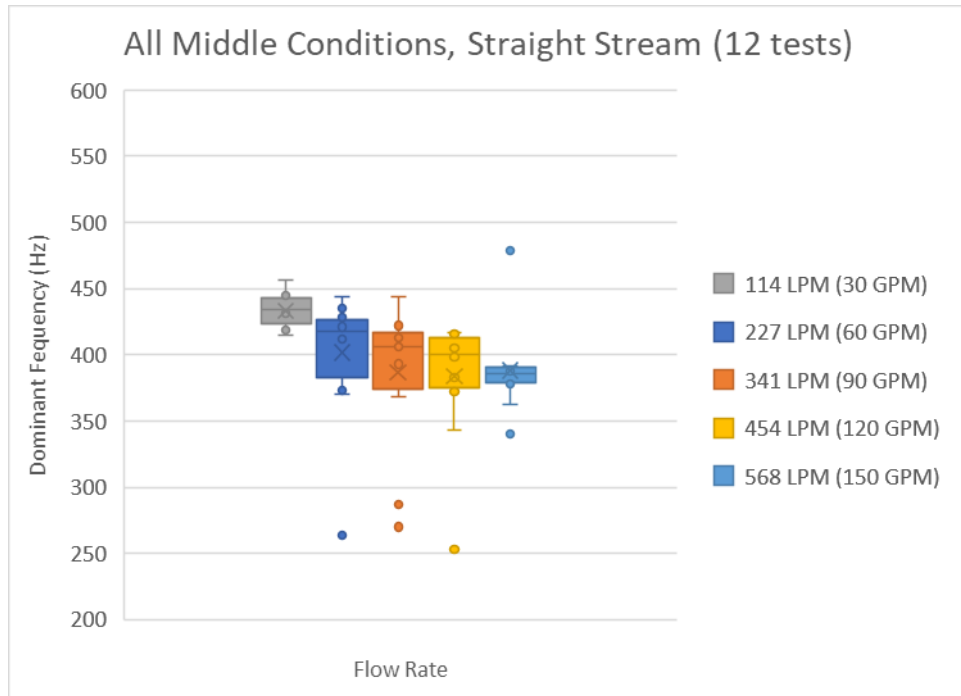


Fig. 28. The dominant frequency for each flow rate with the accelerometer at the middle location for all straight stream experiments.

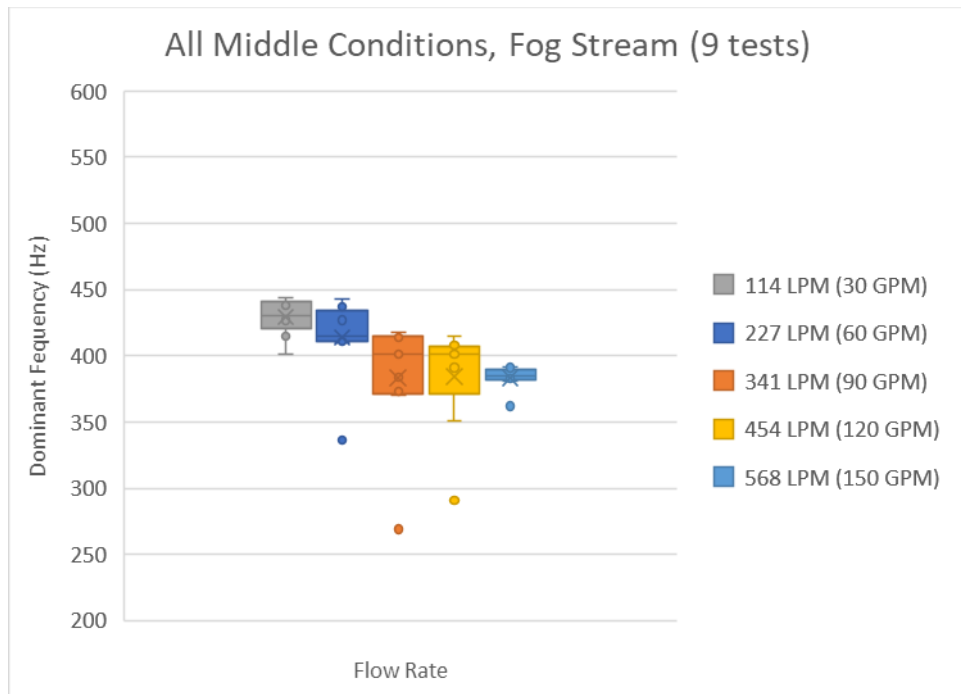


Fig. 29. The dominant frequency for each flow rate with the accelerometer at the middle location for all fog stream experiments.

3.3. Sensor at the Back Hose Location – Stationary on Ground, Dragging, Moving Left and Right

The accelerometer was strapped at the back hose location approximately 2.4 m (8 ft) from the attachment to the water source and the accelerometer was attached to the hose that rested on concrete. The nozzle was elevated off the ground to reduce water flow vibrations between the nozzle and ground that might be detected by the accelerometer, although detection of these vibrations was not expected since the accelerometer was so far from the nozzle.

For the stationary, hose on-ground condition, there were 4 experiments with the straight stream [Fig. 30] and 4 experiments with the fog stream [Fig. 31]. Each experiment included five (5), 1 s, data collection bursts for a total of 20 dominant frequencies for each flow rate for the straight stream and 20 dominant frequencies for each flow rate for the fog stream. Neither the straight stream nor the fog stream had a unique dominant frequency for each flow rate. Variability at several flow rates was high similar to this hose condition at the front and middle hose locations.

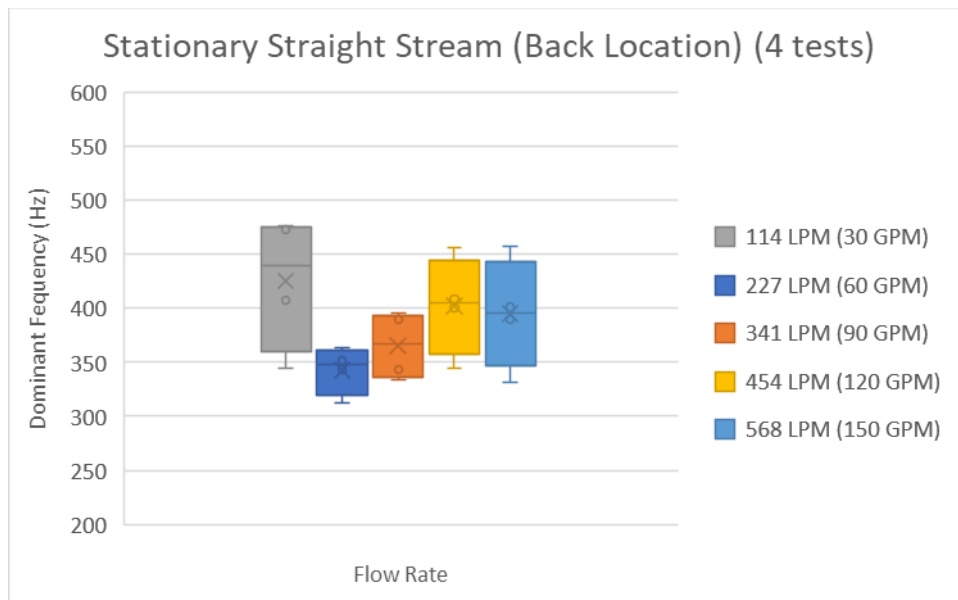


Fig. 30. The dominant frequency for each flow rate with the accelerometer at the back hose location while the hose was stationary on the ground with a straight stream.

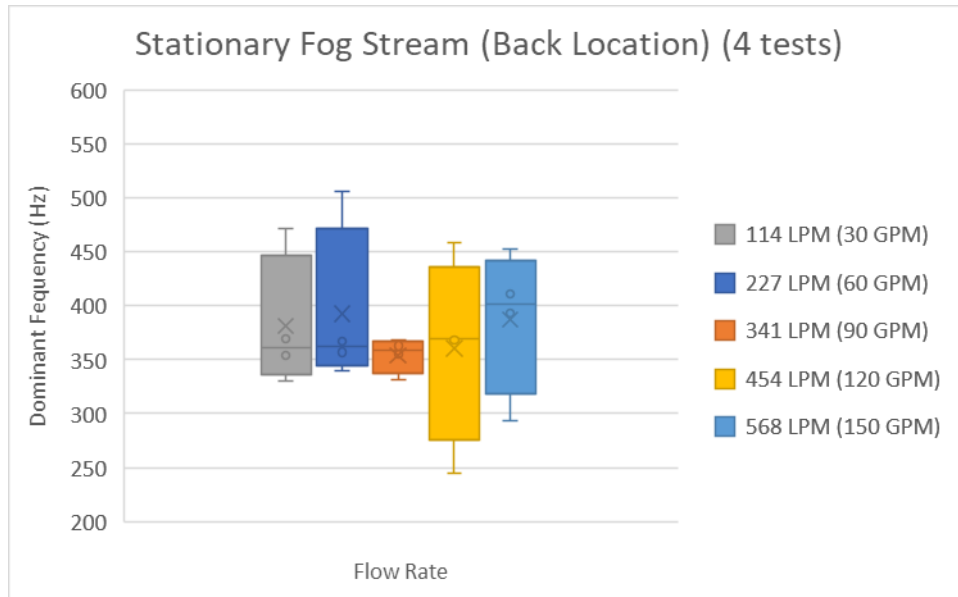


Fig. 31. The dominant frequency for each flow rate with the accelerometer at the back hose location while the hose was stationary on the ground with a fog stream.

For the condition where the hose was moved forward and backward, where the motion was in line with the water flow to simulate dragging, there were 3 experiments with the straight stream [Fig. 32] and 3 experiments with the fog stream [Fig. 33]. Each experiment included five (5), 1 s, data collection bursts for a total of 15 dominant frequencies for each flow rate for the straight stream and 15 dominant frequencies for the fog stream. Neither the straight stream nor the fog stream had a unique dominant frequency for each flow rate. Variability at several flow rates was high unlike the dragging hose condition for the middle hose location.

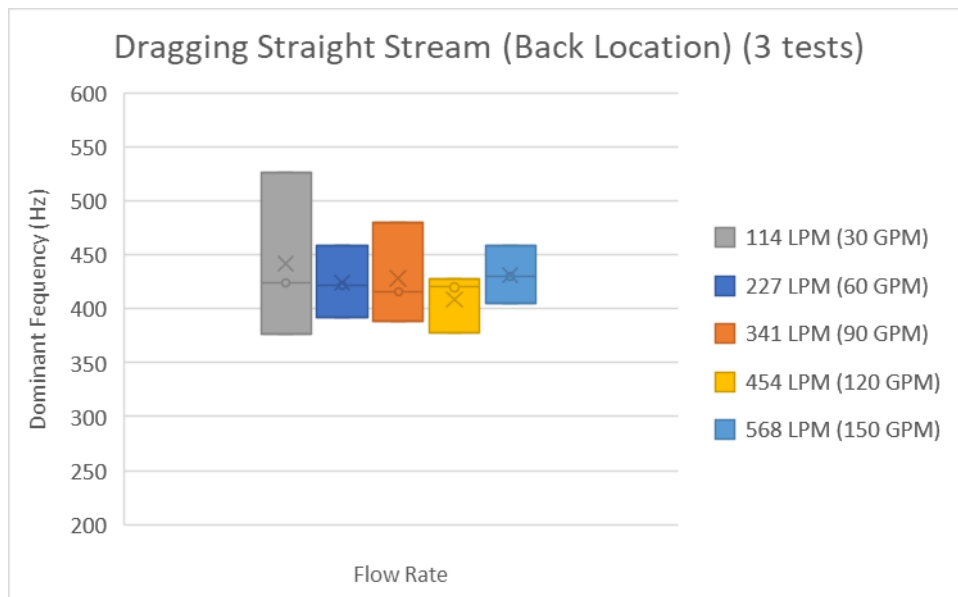


Fig. 32. The dominant frequency for each flow rate with the accelerometer at the back hose location while the hose was moved to simulate dragging on the ground with a straight stream.

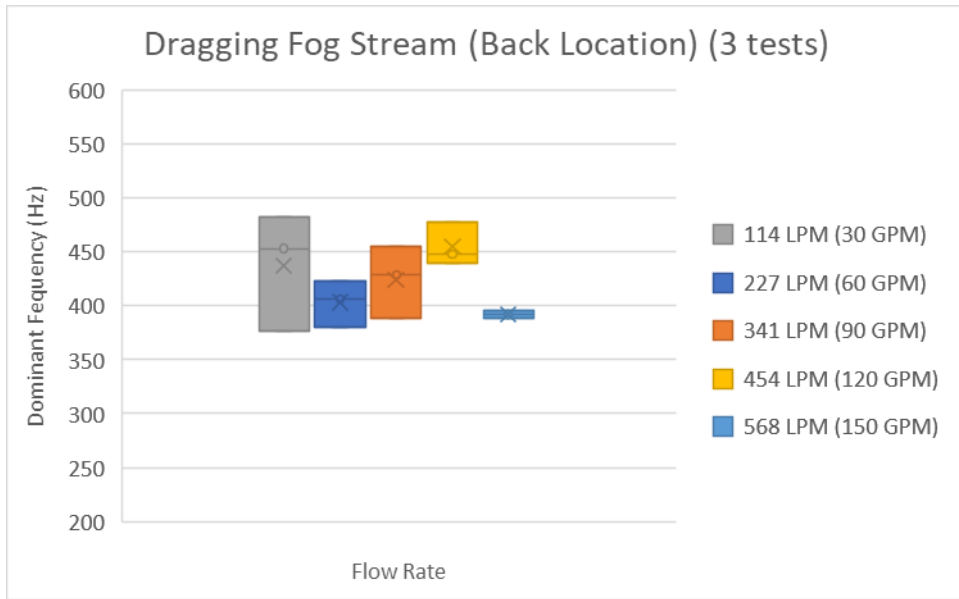


Fig. 33. The dominant frequency for each flow rate with the accelerometer at the back hose location while the hose was moved to simulate dragging on the ground with a fog stream.

For the condition where the hose was moved left and right, perpendicular to the water flow direction, there were 3 experiments with the straight stream [Fig. 34] and 3 experiments with the fog stream [Fig. 35]. Each experiment included five (5), 1 s, data collection bursts for a total of 15 dominant frequencies for each flow rate for the straight stream and 15 dominant frequencies for the fog stream. Neither the straight stream nor the fog stream had a unique dominant frequency for each flow rate. Variability at several flow rates was high unlike moving the hose left and right at the middle hose location.

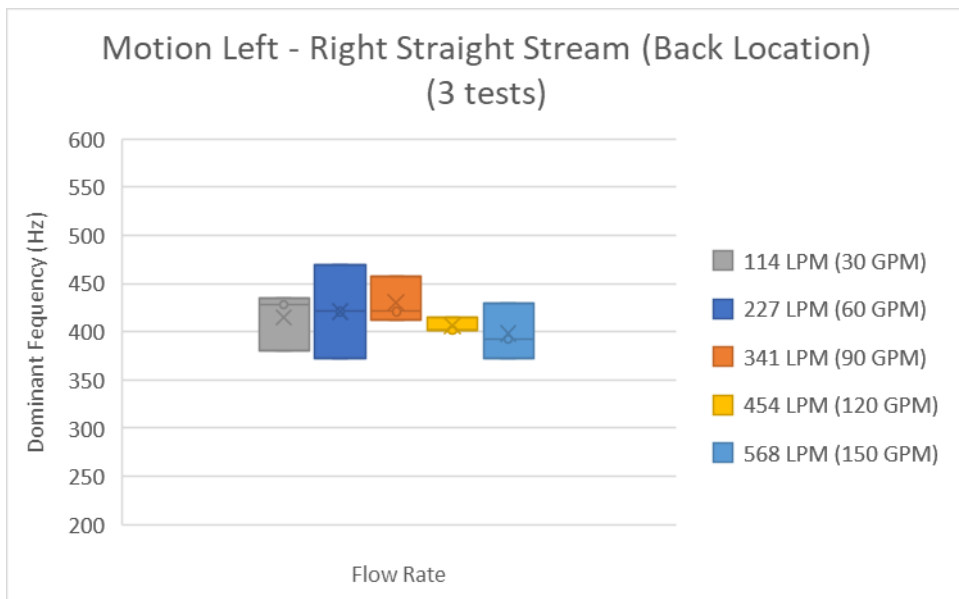


Fig. 34. The dominant frequency for each flow rate with the accelerometer at the back hose location while the hose was moved left and right on the ground with a straight stream.

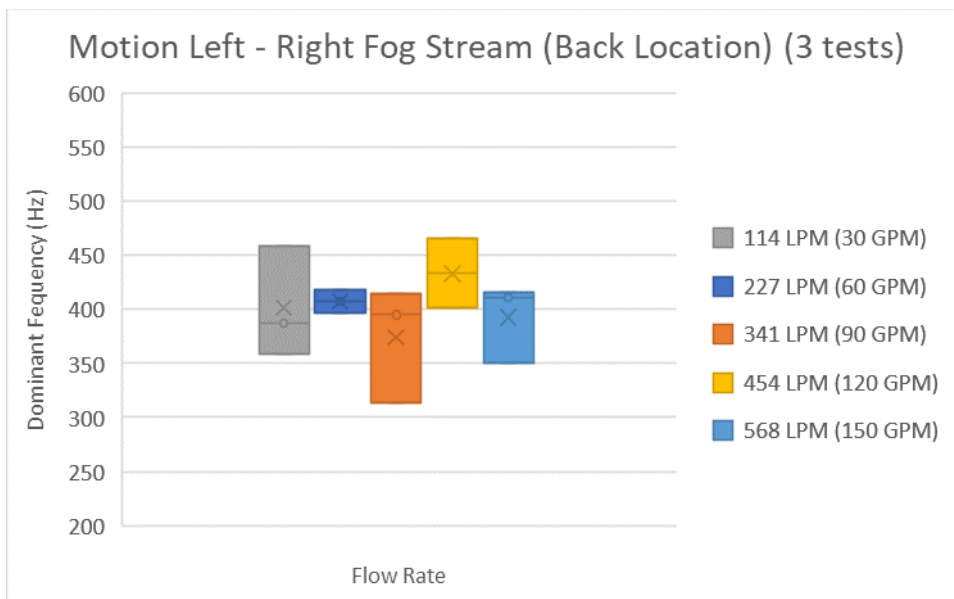


Fig. 35. The dominant frequency for each flow rate with the accelerometer at the back hose location while the hose was moved left and right on the ground with a fog stream.

No further analysis was completed with combined straight and fog stream data because the figures above for the back location showed similar results with high variability.

The back hose location for the accelerometer was the least desirable location to collect data when compared to the front and middle locations, regardless of whether the hose was stationary or in motion. When the accelerometer was attached at the back location, variability in the dominant frequency was high and the average dominant frequency trended up and down over the range of flow rates. This suggests a location dependent difference in the hose vibrations that may be influencing the dominant frequency. The water flowing from the source pipe into the smaller diameter fire hose may have additional vibrations without sufficient time or distance in the hose to settle before passing the accelerometer at the back location.

4. Uncertainty

There were several possible sources of uncertainty in these experiments. The commercial flowmeter specifications report a $\pm 1\%$ accuracy over the flow range for the meter. This accounts for the range of drift in the flow rates from the reference flow meter, mentioned in previous reports, of approximately ± 3.8 LPM (1.0 GPM) at the higher reference flow rates and less drift of approximately ± 1.9 LPM (0.5 GPM) at lower reference flow rates. The fittings upstream and downstream of the reference flow meter may have slightly altered the water flow dynamics as it passed through the turbine affecting the reference flow meter's measurement. The measurement uncertainty from the accelerometers, at the 95% confidence level with coverage factor of 2, was less than $\pm 1.0\%$ for the frequency range used in this study. There was also a likely contribution of uncertainty in our measurements attributed to the fluctuation in the water flow from the water source; the water utility pipes of the building supplied the water to the fire hose. The uncertainty contribution from the water supply was estimated to be approximately

$\pm 3\%$ at the higher flow rates and $\pm 1\%$ at lower flow rates, a larger contribution than the uncertainty from the accelerometers or from the commercial flowmeter.

5. Conclusions

The overall goal of these experiments was to develop a robust, wireless, flow apparatus to measure water flow through a fire hose and communicate the flow to an incident commander to improve firefighting situational awareness. The wireless flow apparatus was used with realistic firefighting hose movements (i.e., holding the hose nozzle, nozzle motion during simulated fire suppression, simulated hose dragging) to evaluate the upgraded apparatus function and determine the influence of the hose motion, sensor location, and hose spray, on the dominant frequency metric.

The sensor unit, including the accelerometer, aluminum alloy base, and plastic cover, was lightweight, easily portable, and small. The separate wireless node however was still large. Neither the sensor unit nor the wireless node is capable of withstanding high temperatures as would be expected on the fire ground, or wet conditions that could compromise the electrical components of the sensor unit or the wireless node. Fireground hardening of the apparatus is still required.

The sensor unit was flexible and easily tightly attached and removed at any location along the fire hose using a Velcro strap. The strap also allows the sensor unit to be attached to different diameter fire hoses or rigid, water suppression, pipes. This was a significant advancement over the previous design where the accelerometer was epoxied to the exterior hose fabric. Based on the results, no loss of vibration signal was observed using the strap.

These experiments continued to show that the wireless flow apparatus was capable of indicating from the hose exterior that water was flowing through a flexible fire hose, however measuring the flow rate was still challenging. In the experiments, although a decreasing trend in dominant frequency with increasing flow rate was observed, a unique dominant frequency was not able to be determined for a given flow rate because of the data variability. One frequency would often correspond to multiple flow rates and therefore, a clear metric for measuring water flow is still undetermined. A GUI via a portable laptop computer was used during the experiments to observe that water was flowing through the fire hose, and the same, or similar, GUI could easily be used by an incident commander.

Some general observations were made from the experiments. The type of hose motion (dragging or fire suppression) did not appear to influence the dominant frequency. Experiments with the sensor elevated above the ground resulted in less variability than experiments with the hose resting on the ground. The hose nozzle stream type, either straight or fog, did not appear to influence the dominant frequency. Variability in the data at the back hose location was greatest and suggests there may be a location dependent difference in the dominant frequency metric for flexible fire hose. The results from these experiments showed improvement of the wireless, flow apparatus hardware, but additional research is still needed to understand the dominant frequency metric.

Further data analysis to evaluate other metrics, or combination of metrics, to determine flow rate may yield an improved relationship for flow rate. An effective field tool to assist the fire service may not require that the flow rate be determined as a value. Knowing that the flow rate is above or below a threshold is still valuable field data to distinguish if water flow rate is sufficient, or whether or not water is flowing at all. The results of these experiments suggest that comparing the dominant frequency of similar flow rates does not result in a unique flow rate. The same dominant frequency often could be interpreted as multiple flow rates. However, in some cases there was a difference between the dominant frequency at the lowest flow rate of 114 LPM (30 GPM) which was often greater than 400 Hz and the highest flow rate of 568 LPM (150 GPM) which was often less than 400 Hz. Although not ideal, a comparison between only the lowest and highest flow rates, using the extreme ends of the dominant frequency curve, could be used to give a no-flow (0 Hz), low-flow (< 400 Hz), or sufficient water flow (> 400 Hz) signal, to improve situational awareness.

6. Future Work

Two areas are considered for future work to advance this project by continuing to evaluate the relationship between the dominant frequency and the flow rate. A wired sensor system, as used previously [1], would allow more vibration data to be collected without the constraints involved using data bursts with the wireless system. A larger volume of data would allow for an improved average acceleration determined for each flow rate. It is possible that this could improve the dominant frequency metric. The dominant frequency results from previous experiments [2] had less variability than the results from the current experiments and additional research is needed to understand the differences. Once the dominant frequency relationship to flow rate is refined with a larger data set, the relationship could then be applied to the more practical smart wireless sensor system to evaluate if it is suitable.

The second area for future work is the application of the best fitting machine learning (ML) model to predict the flow rate based on the dominant frequency metric, or combination of metrics. Existing data would be used to train a ML model and could be supplemented with additional experimental data if more is required. The wired sensor system may be helpful to collect larger data sets for training the model. Lastly, the model's performance would be tested in the field and the robustness evaluated.

References

- [1] Brown CU, Vogl GW, and Tam WC, Measuring Flow Rate for a Fire Hose Using Wired Accelerometers for Smart Fire Fighting, NIST TN 2075, Nov 2019. <https://doi.org/10.6028/NIST.TN.2075>
- [2] Brown, CU, Vogl, GW, and Tam, WC, Measuring Water Flow Rate for a Fire Hose Using a Wireless Sensor Network for Smart Fire Fighting, NIST TN 2074, Nov 2019. <https://doi.org/10.6028/NIST.TN.2074>
- [3] Brown CU, Vogl G, Tam WC (2019) Measuring Water Flow Rate in a Flexible Fire Hose using an Accelerometer. *Suppression, Detection and Signaling Research and Applications Symposium Proceedings (SUPDET)*, Sept 17-19, Denver, CO. (<https://www.nfpa.org/>-

[/media/Files/News-and-Research/Resources/Research-Foundation/Symposia/2019-SUPDET/Presentations/SUPDET19BrownVoglTam-paper.ashx\)](#)

- [4] Brown CU, Vogl GW, Tam WC, Measuring Water Flow Rate for a Fire Hose Using a Wireless Sensor Network for Smart Fire Fighting, Fire Technology (Special Issue on Smart Systems), 57, 3125-3250 (published online Jan 2, 2021).
<https://doi.org/10.1007/s10694-020-01054-1>